

# Tilted $n$ -fold symmetric radio frequency pulse sequences: Applications to CSA and heteronuclear dipolar recoupling in homonuclear dipolar coupled spin networks

J. D. Gross, P. R. Costa, and R. G. Griffin

*Francis Bitter Magnet Laboratory and Department of Chemistry, MIT, Cambridge, Massachusetts 02139*

(Received 8 December 1997; accepted 26 January 1998)

We describe new solid-state NMR methods for measuring the magnitude of the chemical shift anisotropy (CSA) and/or the heteronuclear dipolar coupling in the presence of homonuclear dipolar coupled spin networks under magic-angle spinning (MAS). The techniques employ  $2\pi/5$  phase shifts of a frequency switched Lee–Goldburg irradiation scheme which recouples the CSA and/or the heteronuclear dipolar coupling while simultaneously decoupling the homonuclear dipolar interactions. The induced spin dynamics are sensitive to the magnitude of the CSA and its asymmetry and may be implemented under conditions where the MAS rate exceeds the size of the anisotropic interactions. These approaches could find use in measurements of the magnitudes and relative orientations of CSA and/or heteronuclear dipolar couplings to extract torsion angles in uniformly labeled systems. © 1998 American Institute of Physics. [S0021-9606(98)00717-X]

## INTRODUCTION

Solid-state NMR is an invaluable tool for the study of molecular structure and dynamics. Systems which are difficult to characterize by more conventional techniques, such as x-ray crystallography and solution NMR, provide a strong motivation for the application and further development of NMR methods that accurately measure structural features in the solid state. Furthermore, the anisotropic interactions amongst and between nuclei in rigid solids contain a wealth of information on the bond orientations and interatomic distances. However, in powder samples, these interactions yield broad features and render the spectra of multiple resonances difficult to disentangle.

Special line narrowing techniques such as magic-angle-spinning (MAS)<sup>1,2</sup> and dipolar decoupling<sup>3,4</sup> are capable of producing high resolution spectra rivaling the quality of those obtained in solution NMR, but at the loss of information on anisotropic interactions. There are a number of procedures designed to reintroduce anisotropic interactions within the framework of MAS so that orientation dependent information may be measured with the site resolution provided by the isotropic shift. Specific methods have been designed to recouple the chemical shift anisotropy (CSA)<sup>5–11</sup> in addition to isolated pairs of heteronuclear and homonuclear dipolar coupled spins for quantitative measurements.<sup>12</sup> Ideally, complete isotopic enrichment of molecules with nuclei that are amenable to NMR would provide a route to total structure determination. Unfortunately, the existing methodology is prone to complications arising from strongly homonuclear dipolar coupled spin networks. The dynamics of the recoupled interaction of interest may be influenced or even quenched by incompletely averaged homonuclear dipolar interactions thereby precluding quantitative analysis.<sup>13</sup>

The above problems are particularly acute when measuring heteronuclear dipolar interactions between the rare and

abundant spins. It is well known that such heteronuclear couplings can be measured with reasonable accuracy if measures are taken to decouple the homonuclear dipolar couplings between abundant spins. Most experiments to date are two-dimensional in nature and employ homonuclear decoupling schemes such as MREV-8<sup>14,15</sup> during the indirect dimension where rotational sideband manifolds reflect the strength of the heteronuclear dipolar interaction.<sup>16</sup> The use of such multiple pulse sequences is a quite general approach for measuring CH and NH dipolar couplings and has found recent use in correlating these interactions to measure torsion angles across HCCH<sup>17</sup> and HNCH<sup>18</sup> spin topologies. Unfortunately, as the ratio of spinning speed to dipolar coupling is increased, information on the dipolar interaction is lost. In addition, the efficiency of homonuclear decoupling of the abundant spins is compromised as the cycle time of the MAS approaches that of the multiple pulse sequence.<sup>19</sup> A method has been designed to overcome these shortcomings and has been applied in the context of torsion angle measurements.<sup>20</sup> The advantages of fast MAS (defined here to be when  $\omega_r > \delta/3$ , where  $\delta$  is multiple-pulse scaled dipolar coupling or CSA and  $\omega_r$  is the MAS rate) are clear since both sensitivity and resolution are increased in the directly detected dimension of these experiments. This is due to the fact that under conditions of fast MAS, the intensity of the rotational sidebands is folded into the centerband thereby reducing overlap between sideband manifolds (for the case of multiple sites) while maximizing signal intensities.

A more subtle problem results when attempts are made to measure CSAs in uniformly enriched samples with CSA recoupling schemes developed for noninteracting spin systems. Techniques such as the  $4-\pi$  pulse sequence<sup>10</sup> or rotary resonance recoupling<sup>11,21–23</sup> work well in a natural abundance environment where the dipolar couplings between neighboring spins may be neglected. The introduction of non-negligible dipolar interactions through uniform labeling

poses a problem since most sequences designed to recouple the CSA also recouple both homo- and heteronuclear dipolar couplings. The noncommutation between the recoupled CSA and dipolar interactions introduces dipole-dependent CSA dynamics which often complicate quantitative measurements.

We introduce a radio frequency pulse sequence that simultaneously recouples the heteronuclear dipolar interaction and/or CSA of the irradiated spin while ensuring that the homonuclear dipolar couplings between the irradiated spins are effectively averaged to zero. The techniques utilize the frequency switched Lee–Goldburg (FSLG)<sup>24–26</sup> scheme for homonuclear decoupling. Efficient heteronuclear/CSA recoupling is achieved by employing fivefold symmetric phase shifts<sup>27</sup> of the FSLG scheme over one rotor period. The methods proposed here allow measurement of the CSA and heteronuclear dipolar couplings even when the ratio of spinning speed to dipolar couplings is large. Relatively rapid MAS does not compromise the dipolar decoupling due to the short cycle time of the FSLG scheme. We refer to the methods as Tilted  $C_n$  (TC $n$ ) in analogy with previous sequences proposed by Lee *et al.*<sup>27</sup>

## PHYSICAL PICTURE

The basis of the recoupling schemes presented here is given by the averaging of spin interactions that occurs when a system of spin-1/2 nuclei is exposed to a strong rf field far from resonance. In this case, the rotating frame Hamiltonian may be partitioned

$$H = H_{\text{Int}} + H_{\text{rf,eff}} \quad (1)$$

with

$$H_{\text{rf,eff}} = \Delta \omega I_z + \exp[-i I_z \phi] \omega_1 I_x \exp[i I_z \phi], \quad (2)$$

where the internal part,  $H_{\text{Int}}$ , is given by the spin interactions (the conventional secular terms which commute with  $I_z$ ), and the large external part consisting of the effective rf field,  $H_{\text{rf,eff}}$  containing an offset component parallel to the longitudinal axis of the rotating frame and an rf component in the transverse plane with the phase  $\phi$ . This partitioning of interactions affords a simple physical picture of the effect of the effective field on the spin interactions. The internal Hamiltonian is rotated about the effective rf field at a rate given by the effective field strength. If the effective field is inclined at the magic-angle with respect to the  $z$  axis, the spin operators of  $H_{\text{Int}}$  rotate at the magic-angle [see Fig. 1(a), left]. The homonuclear dipolar coupling, which is characterized as a tensor of rank two with respect to spin rotation, is then averaged to zero (with the proviso that the effective field strength is large relative to the size of the dipolar interactions). This situation of Lee–Goldburg (LG) decoupling<sup>24</sup> can be thought of as magic-angle spinning in “spin space.” In contrast, the chemical shift interactions, tensors of rank one, are only scaled in magnitude with the new direction of the interaction along the effective field [Fig. 1(a), right].

The introduction of magic-angle *sample* spinning does not complicate the above picture provided that the time scales of sample rotation and spin rotation are drastically different. Typically, the size of the effective field may be

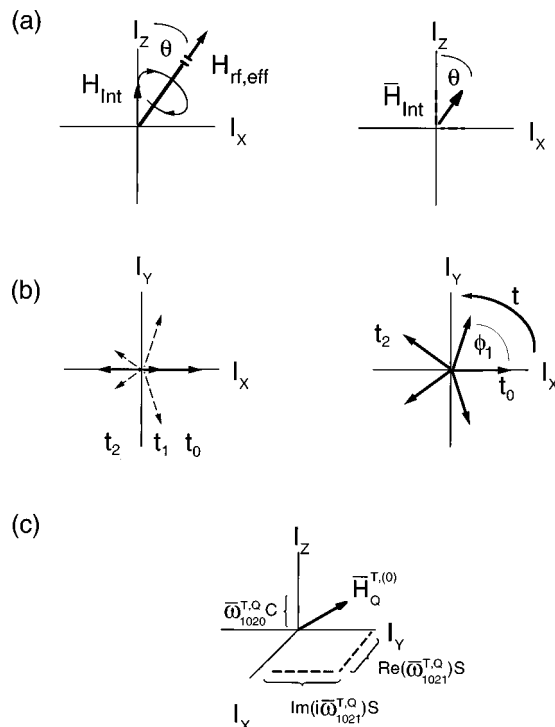


FIG. 1. (a)-left: Direction of the effective rf field in the rotating frame. In a tilted interaction frame defined by the effective rf field, the spin operators are time dependent and rotate about  $H_{\text{rf,eff}}$ , and when  $\theta$  is chosen equal the magic-angle, the homonuclear dipolar coupling is averaged to zero. (a)-right: Rank one interactions are averaged with new direction along the effective field. (b)-left: MAS modulation of the projection of the residual rank one interaction into the transverse plane. Times  $t_0$ ,  $t_1$ , and  $t_2$  and corresponding vectors correspond to different points in MAS cycle. Dashed arrows correspond to the decomposition of the MAS modulation into counter-rotating components. (b)-right: Result of shifting the azimuthal angle,  $\phi$ , of the basic FSLG cycle in steps of  $2\pi/5$  over one rotor period. Change in direction of rf field is coincident with MAS modulation of counter-rotating components and a recoupling is observed (c) Direction of average Hamiltonian for the complete TC $n$  cycle. The coefficients  $C$  and  $S$  correspond to  $\cos(\theta)$  and  $\sin(\theta)$ , respectively. The most efficient recoupling occurs when the effective field is completely transverse (when the isotropic parameters are set to zero or negligible in size relative to the recoupled interactions of interest).

arranged to be at least an order of magnitude greater than the sample spinning speed so that averaging may be considered separately. Although the spin-part of the chemical shift and heteronuclear dipolar coupling transforms as a tensor of rank one, the spatial part of these interactions transforms as a second rank tensor with respect to sample rotation, and the magnitude of the residual chemical shift (and heteronuclear dipolar coupling) are modulated upon the introduction of MAS. It is illustrative to decompose the residual interaction, depicted in Fig. 1(a), into longitudinal and transverse components. The MAS modulation of the residual transverse spin component is depicted in left panel of Fig. 1(b). During the course of a rotor period the size of the component (symbolized by a bold arrow) along the  $x$  axis is sinusoidally modulated. (The MAS modulation of the longitudinal component follows a similar trajectory.) The decomposition of the  $x$  component into counterrotating components (symbolized by dashed arrows) is also depicted. Over one rotor period, the anisotropic interactions are completely averaged leaving be-

hind the unmodulated isotropic components along the  $x$  and  $z$  axis of the rotating frame. Improved averaging through sample and spin rotation has been the basis for several techniques aimed at obtaining high-resolution isotropic chemical shift correlation<sup>28</sup> or optimized coherence transfer schemes in which the deleterious effects of homonuclear dipolar couplings are eliminated.<sup>29–31</sup>

However, it is also possible to reintroduce anisotropic interactions of interest while decoupling the homonuclear dipolar interaction by imposing a second modulation onto the LG (or FSLG) decoupling scheme. For example, the TC $n$  sequences presented here employ  $n$  consecutive  $2\pi/n$  phase shifts of the FSLG cycles within one rotor period. In this case, shifts in the radio frequency phase are manifested as phase shifts of the residual rank 1 spin tensors (chemical shift and heteronuclear dipolar coupling terms). The radio frequency phase shift corresponds to a change in the azimuthal angle orienting the transverse component of the residual spin tensor with respect to the rotating frame [see Fig. 1(b), right]. In this way, the modulation imposed by phase shifting the FSLG cycles interferes with the MAS modulation of residual anisotropic interactions and a “recoupling” is observed. Since the rf phase shifts do not modulate the longitudinal spin component, the anisotropic interactions along the  $z$  axis are averaged by MAS. Similarly, the isotropic terms corresponding to the transverse component are averaged by rf phase shifts since they are not modulated by MAS. Therefore, the recoupled Hamiltonian neatly contains information on isotropic interactions along the  $z$  axis and anisotropic interactions in the transverse plane.

## THEORY

The general scheme for TC $n$  is outlined in Fig. 2(a). Figures 2(b)–2(e) illustrate three possible implementations for measuring heteronuclear dipolar ( $IS$ ) couplings and a single implementation of TC $n$  for CSA recoupling in homonuclear dipolar coupled spin networks. For heteronuclear dipolar recoupling the TC $n$  sequence is applied to the abundant  $I$  spin, typically  $^1\text{H}$ , and  $S$  spin transverse magnetization is allowed to evolve under the recoupled  $IS$  interaction as described below. These experiments may be performed in a one or two dimensional fashion depending on the number of sites to resolve and whether or not refocusing of the  $S$  spin CSA is required. The constant-time implementation refocuses the  $S$  spin chemical shift and is particularly useful when probing multiple sites over a broad spectral range. The rare spin TC $n$  CSA recoupling sequence is depicted in Fig. 2(e) and is strictly two dimensional in nature. The  $\pi/2$  pulse after cross-polarization generates longitudinal magnetization which evolves under the recoupled CSA prior to the  $\pi/2$  pulse required to monitor evolution.

In the following treatment only the irradiated spins are considered: The Hamiltonian consists of the chemical shifts, homonuclear dipolar couplings, and the rf field terms. The results obtained for the recoupled chemical shift will then be extended to cover heteronuclear dipolar interactions. Following the notation in Lee *et al.*,<sup>27</sup> the pulse sequences presented here contain  $n$  subcycles TC $p$  with  $p=0, \dots, n-1$  timed so as to be contained in  $N$  rotor periods. The length of each cycle

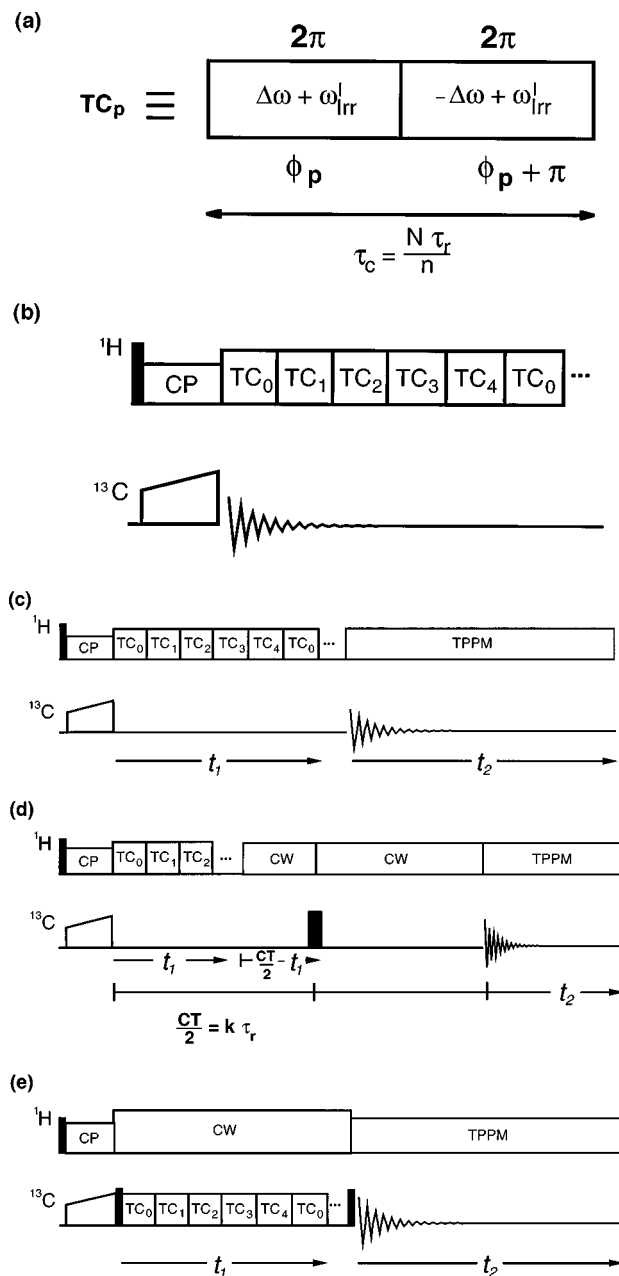


FIG. 2. General scheme for TC $p$  subcycle (a) and pulse sequences for TC $n$  recoupling. (b) One dimensional sequence for measuring heteronuclear interactions. (c) Two dimensional implementations, without isotropic chemical shift refocusing and (d) with constant time implementation. (e) Two dimensional implementation for CSA recoupling. Thin and thick black rectangles correspond to  $\pi/2$  and  $\pi$  pulses, respectively.

$\tau_c$  is  $N\tau_r/n$ , the time required for two  $2\pi$  rotations about the effective rf field,  $\omega_e^I = \sqrt{\Delta\omega^2 + \omega_1^2}$ , with  $\Delta\omega$  as a resonance offset,  $\omega_1$  the nutation frequency, and  $\omega_{\text{Irr}}^I$  left as an adjustable parameter where  $\omega_{\text{Irr}}^I \ll \Delta\omega$ ,  $\omega_1$  [see Fig. 2(a)]. Given the above, the TC $n$  sequences must satisfy the condition  $\omega_e^I = 2n\omega_r/N$ . If the TC $n$  sequence is initiated at time  $t^0$ , the  $p$ th rf cycle TC $p$  runs between time points  $t_p^0$  and  $t_{p+1}^0$  with  $t_p^0 = t^0 + p\tau_c$ . The relevant Hamiltonian for the  $p$ th subcycle, obtained by subsequent transformations where the Hamiltonian is rotated about the  $y$  axis of the rotating frame through the angle  $\theta = \tan^{-1}(\omega_1/\Delta\omega)$  followed by transforma-

tion to an interaction frame defined by the effective rf field, is

$$H^T(t) = \sum_Q \sum_{\lambda\mu lm} \sum_{\mu'} \omega_{\lambda\mu lm}^{T,Q}(t-t_p^0) d_{\mu',\mu}^{(\lambda)}(\theta) \times \exp[i2\pi(Nm - \mu')p/n] V_{\lambda\mu'}^{T,Q} \quad (3)$$

where

$$V_{\lambda\mu'}^{T,Q} = \exp[iI_Y\theta] V_{\lambda\mu'}^Q \exp[-iI_Y\theta] \quad (4)$$

and

$$\omega_{\lambda\mu lm}^{T,Q}(\tau) = \omega_{lm}^Q d_{\mu 0}^{(\lambda)}(-\theta) \exp[i(-1)^S \mu \omega_e^I \tau] \times \exp[im\omega_r(\tau+t^0)] \quad (5)$$

with  $d_{\mu\mu}^{(\lambda)}$  as a reduced Wigner function. The exponent  $S$  in (5) is zero for the first half of the subcycle and unity for the second half, accounting for the inversion of the effective field which occurs every half subcycle. In Eq. (3),  $Q$  references the type of interaction ( $Q=i$  for chemical shift and  $ij$  for the dipolar interaction),  $\lambda$  characterizes the rank of the interaction with respect to spin rotations,  $\mu'$  is the spin rotational component ranging from  $\mu' = -\lambda \dots \lambda$ ,  $l$  is the rank of the interaction with respect to sample rotation and  $m$  is the spatial rotational component ranging from  $m = l, \dots, -l$ .<sup>27</sup> The definitions for the irreducible tensor operators of rank one are given by

$$V_{10}^j = I_{jz} \quad (6)$$

and

$$V_{1\pm 1}^j = \mp 2^{-1/2} I_j^\pm \quad (7)$$

while for rank two tensors

$$V_{20}^{jk} = 6^{-1/2} (3I_{jz}I_{kz} - I_j \cdot I_k), \quad (8)$$

$$V_{2\pm 1}^{jk} = \mp 2^{-1} (I_j^\pm I_{kz} + I_{jz} I_k^\pm), \quad (9)$$

and

$$V_{2\pm 2}^{jk} = 2^{-1} I_j^\pm I_k^\pm \quad (10)$$

with the relevant spatial components defined for the anisotropic chemical shift (assuming axial symmetry for convenience),

$$\omega_{2m}^j = \omega_0 \delta_1^j d_{0m}^{(2)}(\beta_{PR}^j) d_{m0}^{(2)}(\beta_{RL}) \exp(im\gamma_{PR}^j) \quad (11)$$

and dipolar coupling

$$\omega_{2m}^{jk} = 6^{1/2} b_{jk} d_{0m}^{(2)}(\beta_{PR}^{jk}) d_{m0}^{(2)}(\beta_{RL}) \exp(im\gamma_{PR}^{jk}), \quad (12)$$

where  $\delta_1^j \omega_0$  is the chemical shift anisotropy of spin  $j$  and

$$b_{jk} = - \left( \frac{\mu_0}{4\pi} \right) \frac{\gamma_j \gamma_k}{r_{jk}^3} \hbar$$

is the dipolar coupling constant between spins  $j$  and  $k$ . The Euler angles  $\beta_{PR}$  and  $\gamma_{PR}$  correspond to the polar and azimuthal angles of the chemical shift or dipolar coupling tensor in the rotor frame while  $\beta_{RL}$  is the inclination of the rotor with respect to the  $z$  axis of the laboratory frame.

The dynamics of the irradiated spins are calculated using coherent averaging theory.<sup>19</sup> Using the first level of approximation, the zeroth-order average Hamiltonian is calculated first over the  $p$ th subcycle to be

$$\bar{H}_p^{T(0)} = \sum_Q \sum_{\lambda\mu lm} \sum_{\mu'} \bar{\omega}_{\lambda\mu lm}^{T,Q} d_{\mu',\mu}^{(\lambda)}(\theta) \times \exp[i2\pi(Nm - \mu')p/n] V_{\lambda\mu'}^{T,Q} \quad (13)$$

with the amplitude

$$\bar{\omega}_{\lambda\mu lm}^{T,Q} = \tau_c^{-1} \int_0^{\tau_c} \omega_{\lambda\mu lm}^{T,Q}(\tau) d\tau. \quad (14)$$

Equation (13) illustrates the response of the spatial and spin rotational components to the phase shifts of the rotor and rf between successive subcycles of the pulse sequence. For the TCn sequences a relationship linking the symmetry numbers of the tilted pulse sequence ( $N, n$ ) with the rotational components ( $\mu', m$ ) may be derived by calculating the zeroth-order average Hamiltonian over the total cycle through

$$\begin{aligned} \bar{H}^{T(0)} &= n^{-1} \sum_{p=1}^{n-1} \bar{H}_p^{T(0)} \\ &= \sum_Q \sum_{\lambda\mu lm} \sum_{\mu'} \bar{\omega}_{\lambda\mu lm}^{T,Q} d_{\mu',\mu}^{(\lambda)}(\theta) V_{\lambda\mu'}^{T,Q} E[(Nm - \mu')/n], \end{aligned} \quad (15)$$

where the function  $E(x)$  is unity if  $x$  is an integer or zero otherwise. The function  $E(x)$  in Eq. (15) results from the fact that interactions which survive the average over a subcycle are further modulated by the index,  $(Nm - \mu')/n$  through Eq. (13). If the index is equal to an integer, a stationary term results, the corresponding interaction survives the final average, and a recoupling effect is observed.

If  $\omega_e^I \gg \omega_r$ ,  $|d_{\mu 0}^{(\lambda)}(-\theta) \omega_{lm}^Q|$ :

$$\bar{\omega}_{\lambda\mu lm}^{T,Q} = \delta_{\mu 0} \tau_c^{-1} \int_0^{\tau_c} \omega_{\lambda\mu lm}^{T,Q}(\tau) d\tau, \quad (16)$$

and in this case, Eq. (13) takes the form:

$$\bar{H}^{T(0)} = \sum_Q \sum_{\lambda\mu' lm} \bar{\omega}_{\lambda 0 lm}^{T,Q} d_{\mu',0}^{(\lambda)}(\theta) V_{\lambda\mu'}^{T,Q} E[(Nm - \mu')/n]. \quad (17)$$

In this limit, if  $\theta$  is chosen to be the magic-angle,  $\bar{\omega}_{\lambda 0 lm}^{T,Q} = 0$  for  $\lambda = 2$ , and the homonuclear dipolar interactions are eliminated to zeroth-order over the individual subcycles. This result is expected as each subcycle represents the FSLG sequence applied with a different azimuthal angle,  $\phi$ , of the effective field. The rotational symmetry of the Hamiltonian requires that the FSLG decoupling be invariant to  $\phi$  as is demonstrated here. Equally important is the fact that the amplitude (14) corresponding to the chemical shift and heteronuclear dipolar interactions (both  $\lambda = 1$ ) is not drastically reduced for  $\theta = 54.74^\circ$ . In contrast if  $\theta = 90^\circ$  the homonuclear dipolar interactions ( $\lambda = 2$ ) are scaled by  $-1/2$  while

TABLE I. Symmetry table for  $\mu' = \pm 1$  and  $N=1$  rotor period.

$m$	$\mu' = \pm 1$	$Nm - \mu'$
2	+	1
	-	3
1	+	0
	-	2
0	+	-1
	-	1
-1	+	-2
	-	0
-2	+	-3
	-	-1

the shifts and heteronuclear interactions are reduced to near zero over a subcycle as in the sevenfold symmetric sequence (C7).<sup>27</sup>

In the C7 sequence the symmetry numbers of the pulse sequence ( $N, n$ ) are chosen such that  $N=2$  and  $n=7$  so that the residual chemical shift anisotropy is averaged over the total cycle while only the components  $(\mu', m) = 2, 1$  and  $-2, -1$  are selected for efficient double quantum recoupling. In general, the average Hamiltonian may be engineered so that the recoupled interaction contains a reduced orientational dependence if the symmetry numbers,  $N$  and  $n$ , are chosen such that only terms for which  $(\mu', m)$  and  $(-\mu', -m)$  survive the total average through Eq. (15). When the homonuclear dipolar interactions are effectively decoupled the remaining  $\mu' = \pm 1$  terms correspond to the CSA and heteronuclear dipolar coupling. The scaling of the recoupled interactions is minimized by choosing the  $m=1$  component. Accordingly, for  $N=1$  rotor period, the  $(\mu', m) = (1, 1)$  and  $(-1, -1)$  components are selected if  $n > 3$  (see Table I). [For  $N=2$  rotor periods,  $(\mu', m) = 1, 1$  and  $-1, -1$  are selected only if  $n=5$ .] The final result, expressed in the rotating frame, for  $N=1$ ,  $n=5$ , including both the chemical shift and heteronuclear dipolar coupling is

$$\begin{aligned} \bar{H}^{T(0)} = & \left[ \bar{\omega}_{1020}^{T,I} \cos \theta I_Z + \bar{\omega}_{1021}^{T,I} \frac{\sin \theta}{2} I^+ + \bar{\omega}_{102-1}^{T,I} \frac{\sin \theta}{2} I^- \right] \\ & + 2 \left[ \bar{\omega}_{1020}^{T,IS} \cos \theta I_Z + \bar{\omega}_{1021}^{T,IS} \frac{\sin \theta}{2} I^+ \right. \\ & \left. + \bar{\omega}_{102-1}^{T,IS} \frac{\sin \theta}{2} I^- \right] S_Z. \end{aligned} \quad (18)$$

The isotropic terms are  $\bar{\omega}_{1020}^{T,IS} = \pi J_{IS} \cos \theta$ , the scaled heteronuclear  $J$  coupling, and  $\bar{\omega}_{1020}^{T,I} = 2\pi \bar{\delta}_0^I \cos \theta$ , the average offset from resonance (mean offset), where  $\bar{\delta}_0^I$  is defined as the sum of the mean frequency of irradiation,  $\bar{\omega}_{\text{irr}}^I/2\pi$ , and the offset of the rf carrier from the  $I$  spin resonance ( $\delta_0^I$ ) in the absence of irradiation. The recoupled anisotropic interactions are written

$$\begin{aligned} \bar{\omega}_{1021}^{T,Q} = \bar{\omega}_{102-1}^{T,Q*} = & -C^Q \frac{15}{16\pi} \cos \theta \sin 2\beta_{PR} \\ & \times \sin 2\beta_{RL} \{ \exp[-i\pi/10] + i \} \\ & \times \exp[i(\omega_r t^0 + \gamma_{PR}^0)] \end{aligned} \quad (19)$$

with the definitions  $C^{IS} = b_{IS}$  and  $C^I = \delta_1^I \omega_0$ . The direction of average Hamiltonian (18), defined by the relationship between spin components in the rotating frame, is determined by the isotropic parameters in addition to the angle  $\gamma_{PR}$  [see Fig. 1(c)]. In general the direction of the effective fields corresponding to the chemical shift and dipolar coupling terms in (18) will not be parallel resulting in noncommuting spin interactions. In this case the dynamics would depend on the isotropic parameters in addition to the size and relative orientation of the CSA and dipolar coupling tensors. However, the mean offset may be set to zero and, neglecting the scalar coupling, the outstanding issue is the relative alignment between the principle axis systems of the chemical shift and dipolar tensors since the remaining terms in Eq. (18) do not commute with each other for different phase angles  $\gamma_{PR}$ . In the case of CSA recoupling, any heteronuclear dipolar couplings that are simultaneously reintroduced may be decoupled. For the case of  $^{13}\text{C}-^1\text{H}$  recoupling where  $^1\text{H}$  is irradiated, it is safely assumed that the CSA does not effect the dynamics since the magnitude of the  $^{13}\text{C}-^1\text{H}$  dipolar interaction is typically an order of magnitude larger. Thus for the most interesting cases it is possible to arrange matters so that the CSA and dipolar recoupling may be performed independently. For  $\theta = \beta_{RL} = \tan^{-1} \sqrt{2}$ , the magnitude of the recoupled interaction is written

$$|\bar{H}_Q^{T(0)}| = C^Q \frac{5\sqrt{2}}{24\pi} \sqrt{5-\sqrt{5}} \sin 2\beta_{PR} \quad (20)$$

with  $Q=I$  or  $IS$  assuming the isotropic parameters,  $\bar{\omega}_{1020m}^{T,Q}$ , are zero. The anisotropic interactions are scaled by 0.15 from their static value and the magnitude of the recoupled interaction is independent of  $\gamma_{PR}$ .

## EXPERIMENTAL AND NUMERICAL PROCEDURES

All experiments were performed on a 9.4 T magnet equipped with a custom-built spectrometer console and HCN triple resonance transmission line probe. The spinning rates were either 8 or 10 kHz (controlled to within 2 Hz) and in all cases ramped cross polarization<sup>32</sup> was employed to increase sensitivity and to ensure reproducibility of signal enhancements over long time scales. For the TC5 sequence presented here, the tilt angle was 54.74°. Accordingly, the offset and nutation frequency were chosen to satisfy,  $\theta = \tan^{-1}(\omega_1/\Delta\omega)$ , and produce an effective field that is 10 times the spinning speed. The mean frequency of irradiation was varied empirically by adjusting the parameter  $\omega_{\text{irr}}^I/2\pi$  in steps of 1 kHz, in order to optimize recoupling efficiency (see Discussion below.) The TPPM decoupling scheme was employed during acquisition<sup>4</sup> (where applicable) with rf field strengths of 80 kHz,  $\phi = 10$  or  $15^\circ$ , and  $\tau_p = 5.8 \mu\text{s}$ . CW decoupling was utilized during the  $t_1$  period of the TC5 CSA recoupling sequences with a field strength of 125 kHz to avoid signal losses due to interference between CW decoupling and TC5 mixing. For the 2D experiments, 64  $t_1$  points were collected by incrementing the evolution period in units of one subcycle. The resulting data were zero-filled to 512 points prior to real 2D Fourier transformation. In all

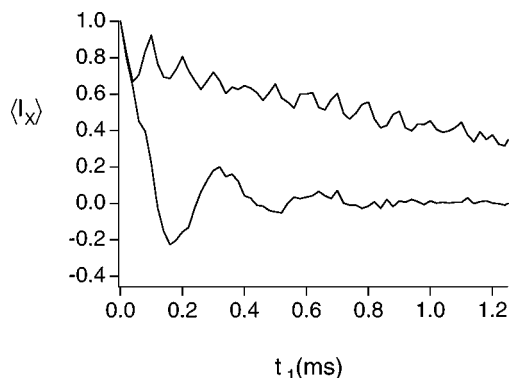


FIG. 3. Experimental results for TC5 CH recoupling ( $N=1$ ) for  $^{13}\text{C}$  enriched  $\text{C}_\alpha$  alanine obtained with sequence depicted in Fig. 2(c) Top trace: FSLG control experiment, obtained with  $\phi_p$  as a constant phase 0. Bottom trace: obtained with  $2\pi/5$  phase shifts of basic FSLG subcycle (b). Experimental conditions:  $\omega_r/2\pi=10.0$  kHz,  $\delta'_0<|1|$  kHz,  $\omega_1/2\pi=81.65$  kHz,  $\Delta\omega/2\pi=57.73$  kHz,  $\bar{\omega}_{1r}^1/2\pi=5.0$  kHz,  $B_0=9.4$  T.

cases 10 and 100 Hz of line broadening were added to the direct and indirect dimensions, respectively. The nutation frequency employed was measured from a  $2\pi$  pulse length.

Numerical lineshape simulations were performed using a program written in C that computes the spin dynamics of an  $\text{IX}_2$  system of spin-1/2 nuclei exposed to MAS and an arbitrary rotor synchronized pulse cycle. Numerical integration of the equations of motion<sup>33</sup> are achieved through standard methods and powder averaging was performed using the method of Cheng and Suzukawa.<sup>34</sup> For each crystal orientation, the propagator was calculated over one rotor period. The cyclic nature of the rf pulse sequence and the periodicity of MAS allow the time development of the initial condition to be evaluated by successive application of the propagator. Time domain data corresponding to each crystal orientation were weighted and coadded prior to real Fourier transformation for numerical line shape analysis.

## RESULTS AND DISCUSSION

Results demonstrating the effectiveness of the TC5 recoupling sequence on  $^{13}\text{C}_\alpha$  labeled alanine (obtained from Cambridge Isotope Labs, Woburn MA) are depicted in Fig. 3. These data were acquired with the application of the sequence depicted in Fig. 2(c). The top curve was acquired with FSLG irradiation and serves as a control since minimal decay should be observed in the limit of efficient homonuclear decoupling. As expected, small amplitude rotational echoes are observed since the spinning speed is very near the FSLG scaled dipolar coupling. Upon introduction of the  $2\pi/5$  phase shifts between subsequent FSLG subcycles, strong oscillations occur due to the recoupled  $^{13}\text{C}-^1\text{H}$  interaction as depicted in the bottom trace. A real Fourier transformation of the data illustrates the contrast in information content between the low amplitude rotational sidebands produced by free evolution under fast MAS and recoupled powder line shape obtained upon application of TC5 [see Figs. 4(a) and 4(b)]. The full-width-at-half-height (FWHH) of the spectrum displayed in Fig. 4(a) is on the order of several hundred Hz (see below) and places a lower limit on the ef-

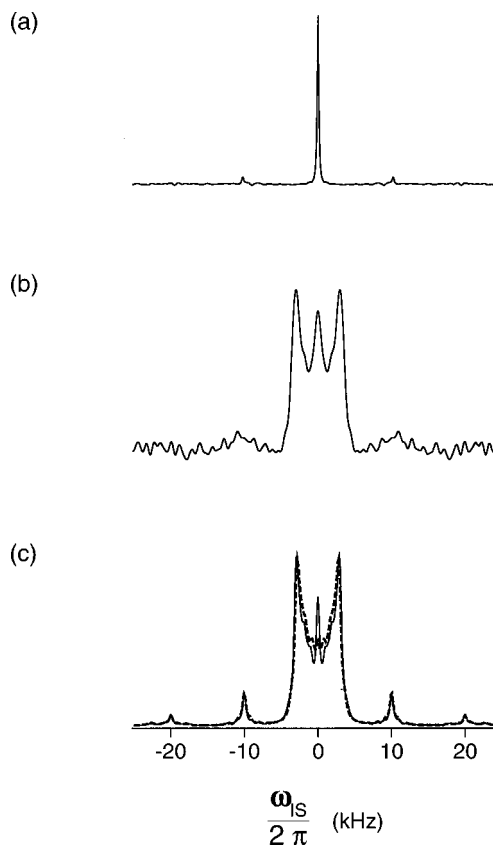


FIG. 4. Comparison of experimental data from Fig. 3 with numerical lineshape simulations. (a) Real Fourier transform of FSLG control experiment. (b) Real Fourier transform of experimental data from TC5 on  $^{13}\text{C}$  enriched  $\text{C}_\alpha$  alanine and (c) numerical lineshape simulations with (solid line) and without (dashed line) mean offset. Simulation parameters on three spin system  $\text{CH}_a$  with remote proton  $\text{H}_b$ :  $\omega_r/2\pi=10.0$  kHz,  $\delta'_{0,a}=0$  or 1 kHz,  $\delta'_{0,b}=2$  kHz,  $\bar{\omega}_{1r}^1/2\pi=0$ ,  $\omega_1/2\pi=81.65$  kHz,  $\Delta\omega/2\pi=57.73$  kHz,  $b_{1Sa}=20.3$  kHz,  $b_{1Sb}=3$  kHz,  $\delta'_{1,a}=\delta'_{1,b}$  2.25 ppm with Euler angles  $\{\alpha_{PC}, \beta_{PC}, \gamma_{PC}\}$ :  $\{0, 109.5, 0\}$ ;  $\{0, 60, 0\}$ ;  $\{0, 109.5, 0\}$ ;  $\{0, 60, 0\}$ , respectively, and  $B_0=9.4$  T.

fectiveness of FSLG decoupling of the  $^1\text{H}-^1\text{H}$  dipolar interactions in alanine. Furthermore, numerical line shape simulations of FSLG decoupling under the conditions presented here indicate that a FWHH well under 1 ppm is obtainable with  $^1\text{H}-^1\text{H}$  dipolar couplings as large as 10 kHz (data not shown). These observations confirm the efficiency of FSLG decoupling when the effective field is ten times the spinning speed and sufficiently larger than the  $^1\text{H}$  homonuclear dipolar couplings, validating the approximation inherent in Eqs. (16)–(17).

Fits of the experimental lineshapes with numerical lineshape simulations are presented in Fig. 4. The dashed line in Fig. 4(c) is a simulation for a model three spin system consisting of a  $^{13}\text{C}-^1\text{H}_a$  group dipolar coupled to a remote proton  $^1\text{H}_b$ . There is good agreement between the splitting observed in the experimental data with that given by the idealized simulations. The solid line in Fig. 4(c) was taken using the same simulation parameters as the dashed line but with the inclusion of a 1 kHz mean offset. The central peak results from inefficient recoupling of crystallites oriented so as to have weak dipolar couplings where the dynamics are quenched by a finite mean offset. The orthogonality between

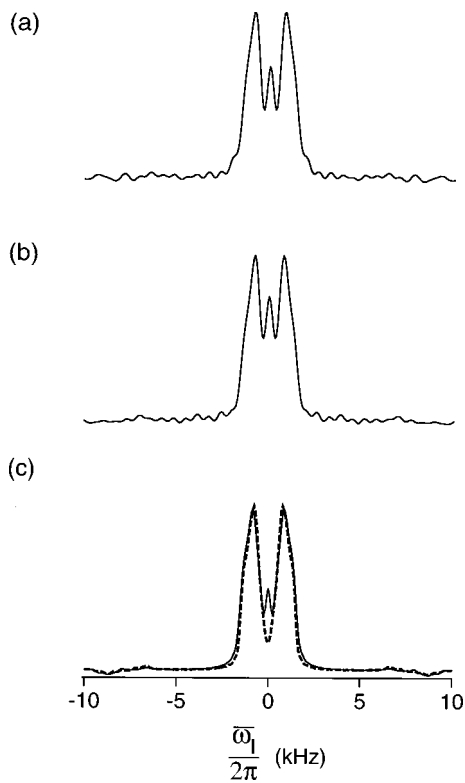


FIG. 5. Comparison of experimental data corresponding to the carboxylate region for (a) natural abundance glycine and (b)  $^{13}\text{C}, ^{15}\text{N}$  glycine under TC5 ( $N=1$ ) CSA recoupling sequence depicted in Fig. 2(e) with numerical lineshape simulations (c). Experimental conditions  $\omega_r/2\pi=8.0$  kHz,  $\delta'_0=0.5$  kHz,  $\omega_1/2\pi=65.32$  kHz,  $\Delta\omega/2\pi=46.18$  kHz,  $\bar{\omega}_{\text{irr}}^1/2\pi=1.0$  kHz and  $B_0=9.4$  T. Numerical lineshape simulations performed with (solid line) and without (dashed line) mean offset. Simulation parameters:  $\omega_r/2\pi=8.0$  kHz,  $\delta'_0=0$  or 0.5 kHz,  $\omega_1/2\pi=65.32$  kHz,  $\Delta\omega/2\pi=46.18$  kHz,  $\bar{\omega}_{\text{irr}}^1/2\pi=0$  kHz,  $\delta'_1=73$  ppm,  $\eta^1=0.93$ , and  $B_0=9.4$  T.

spin components corresponding to the mean offset and the anisotropic interactions in the effective Hamiltonian (18) indicates that the dynamics are dependent on the mean offset and may be quenched entirely in the limit where the scaled mean offset is large relative to the size of the recoupled anisotropic interactions.

Experimentally, the central peak remains even if measures are taken to ensure that the mean offset is zero. Empirical optimization of the recoupling efficiency is achieved by minimizing the central peak through adjustment of the mean frequency of irradiation,  $\bar{\omega}_{\text{irr}}^1$ . Although the resonance offset,  $\delta'_0$ , of  $\text{H}_\alpha$  in alanine was within 1 kHz, optimal recoupling was observed when the frequency switching took place between 62.73 and  $-52.73$  kHz which represents a shift of  $+5$  kHz from the nominal values of  $\pm 57.73(\pm 1)$  kHz for  $\Delta\omega$ . Numerical simulations indicate that a misadjustment of the nutation frequency from its nominal value results in such a central peak. (Data not shown.) Others have observed that displacements of the mean frequency in FSLG decoupling improve the decoupling performance suggesting a second averaging of pulse errors.<sup>25,26</sup> It may be that a slight departure of the mean frequency from the nominal value is necessary to compensate for rf inhomogeneity or phase transients which would be deleterious for both  $^{13}\text{C}$ - $^1\text{H}$  recoupling and  $^1\text{H}$ - $^1\text{H}$  decoupling.

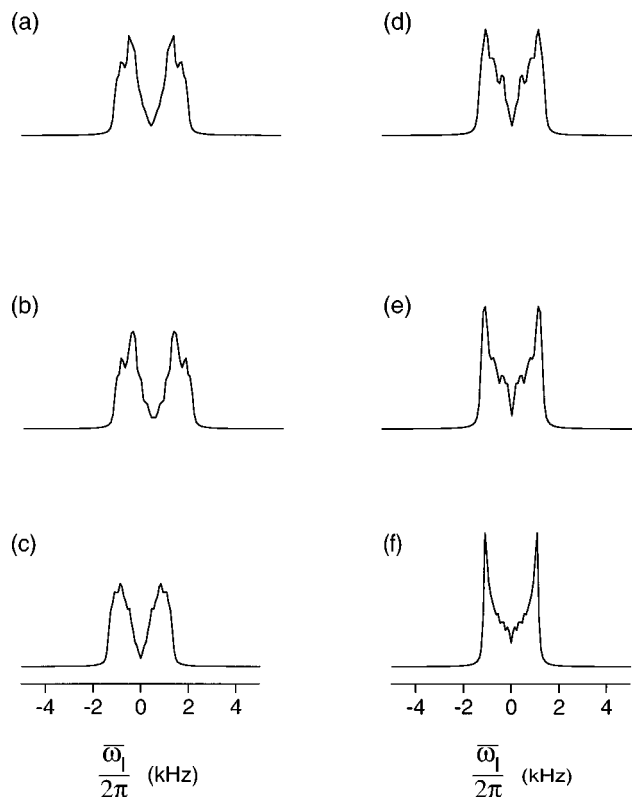


FIG. 6. Numerical lineshape simulations of TC5 ( $N=1$ ) CSA recoupling depicting dependence of recoupled powder lineshape on asymmetry parameter,  $\eta^1$ . Simulation parameters:  $\omega_r/2\pi=12.5$  kHz,  $\delta'_0=0$  kHz,  $\omega_1/2\pi=102.1$  kHz,  $\Delta\omega/2\pi=72.2$  kHz,  $\bar{\omega}_{\text{irr}}^1/2\pi=0$  kHz,  $\delta'_1=73$  ppm, and  $B_0=9.4$  T. In (a)–(f)  $\eta^1$  is equal to 1.0, 0.8, 0.6, 0.4, 0.2, and 0.0, respectively.

The chemical shift anisotropy may be recoupled and measured accurately in the presence of homonuclear dipolar coupled spins using the sequence in Fig. 2(e). Samples of natural abundance and fully  $^{13}\text{C}, ^{15}\text{N}$  labeled glycine (obtained from CIL) were recrystallized prior to NMR experiments. Experimental results using the TC5 sequence of Fig. 2(e) with a MAS rate of 8 kHz are depicted in Fig. 5 for the carbonyl group of glycine. Clearly there is good agreement between the recoupled powder lineshape corresponding to natural abundance glycine in Fig. 5(a) with fully labeled glycine in Fig. 5(b). Numerical lineshape simulations using an anisotropy of 73.0 ppm and  $\eta=0.93$ <sup>35</sup> show excellent agreement with the experimental data. Again, the experimental recoupling efficiency was optimized empirically by varying the mean frequency of the TC5 irradiation so as to minimize the central peak intensity. The mean frequency employed was approximately 1.0 kHz greater than the nominal value. Although an axially symmetric CSA was assumed during the theoretical treatment for sake of brevity [see Eq. (11)], the lineshapes obtained through the TC5 experiment are sensitive to both the magnitude of the anisotropy and the asymmetry parameter as depicted in Figs. 6(a)–6(f). Unfortunately, the experiment is insensitive to the sign of the anisotropy due the intrinsic symmetry of the recoupled powder lineshapes.

Within the framework presented here, where a single irradiation scheme is employed for recoupling of CSA/heteronuclear dipolar interactions, efficient recoupling may

take place with the symmetry numbers  $N=1$  and  $n>3$  or  $N=2$  and  $n=5$ . These conditions may offer potential advantages because the demands on rf power are smaller. Specifically, for TC4 and TC5 ( $N=2$ ) the effective field must be either 8 or 5 times the spinning speed, respectively. If the rf power requirement for effective decoupling of the homonuclear interactions is modest, such as in the application of  $^{13}\text{C}$  CSA recoupling, then the above conditions would offer an advantage for the measurement of smaller CSAs in the case where efficient  $^1\text{H}$  decoupling during mixing is required. It is well known that signal loss results during mixing sequences when efforts are not made to avoid a mismatch between the rf power levels of the mixing scheme and CW  $^1\text{H}$  decoupling.<sup>36,37</sup> Symmetry numbers which result in lower effective field requirements would allow the appropriate mismatch between the  $^1\text{H}$  decoupling and CSA recoupling sequence that would minimize signal loss from inefficient  $^1\text{H}$  decoupling. In addition, for the case of a fixed effective field direction, lower effective field strengths correspond to smaller nutation frequencies which would translate into a smaller contribution of rf field inhomogeneity errors, and the increased time required to achieve  $2\pi$  rotation could potentially reduce the contribution of phase transient errors to the dynamics.

## CONCLUSION

The proposed methods contain a general scheme for efficient CSA/heteronuclear dipolar recoupling in the presence of homonuclear dipolar coupled spin networks. The magnitude of the anisotropic interactions may be extracted from recoupled powder line shapes by numerical line shape simulations, and for the case of CSA recoupling, the line shape is sensitive to the symmetry parameter. The methods represent an improvement over previous techniques since the dynamics of the recoupled interaction are completely separated from the homonuclear interactions through efficient dipolar decoupling. An additional advantage is realized since measurements may be made under conditions of fast MAS thereby increasing sensitivity and resolution. Application of TC4 or TC5 recoupling should allow experiments that measure torsion angles across HCCH<sup>17</sup> or HNCH<sup>18</sup> spin topologies to be implemented at higher spinning rates. In addition, the approaches presented here should allow for the measurement of torsion angles via CSA correlation in uniformly enriched samples. Although the sequences presented here are single irradiation schemes, it is possible to extend the TC $n$  principle to double irradiation schemes which would allow for generation of heteronuclear multiple quantum coherence in a fashion that is independent of HH (or CC) dipolar couplings which would be useful in applications of 2D  $^1\text{H}$ - $^{13}\text{C}$  chemical shift correlation.

## ACKNOWLEDGMENTS

This research was supported by the National Institutes of Health (GM-23403, NS-AG14366, and GM-23289, and RR-00995). The authors would like to thank Chad Rienstra and Dr. Marc Baldus for stimulating discussions throughout the course of this work.

- <sup>1</sup>E. R. Andrew, A. Bradbury, and R. G. Eades, *Nature (London)* **182**, 1659 (1958).
- <sup>2</sup>M. M. Maricq and J. S. Waugh, *J. Chem. Phys.* **70**, 3300 (1979).
- <sup>3</sup>J. Schaefer and E. O. Stejskal, *J. Am. Chem. Soc.* **98**, 1031 (1976).
- <sup>4</sup>A. E. Bennett, C. M. Rienstra, M. Auger, K. V. Lakshmi, and R. G. Griffin, *J. Chem. Phys.* **103**, 6951 (1995).
- <sup>5</sup>M. A. Alla, E. I. Kundla, and E. T. Lippmaa, *JETP Lett.* **27**, 194 (1978).
- <sup>6</sup>Y. Yarmin-Agaev, P. N. Tutjian, and J. S. Waugh, *J. Magn. Reson.* **47**, 51 (1982).
- <sup>7</sup>A. Bax, N. M. Szevereni, and G. E. Maciel, *J. Magn. Reson.* **55**, 494 (1983).
- <sup>8</sup>W. P. Aue, D. J. Ruben, and R. G. Griffin, *J. Chem. Phys.* **80**, 1729 (1984).
- <sup>9</sup>E. T. Olejniczak, S. Vega, and R. G. Griffin, *J. Chem. Phys.* **81**, 4804 (1984).
- <sup>10</sup>R. Tycko, G. Dabbagh, and P. A. Mirau, *J. Magn. Reson.* **85**, 265 (1989).
- <sup>11</sup>Z. Gan and D. M. Grant, *Chem. Phys. Lett.* **168**, 304 (1990).
- <sup>12</sup>A. E. Bennett, R. G. Griffin, and S. Vega, *NMR Basic Principles Progr.* **33**, 1 (1994).
- <sup>13</sup>P. R. Costa, B. Q. Sun, and R. G. Griffin (in preparation).
- <sup>14</sup>P. Mansfield, M. J. Orchard, D. C. Stalker, and K. H. B. Richards, *Phys. Rev. B* **7**, 90 (1970).
- <sup>15</sup>W. K. Rhim, D. D. Elleman, and R. W. Vaughan, *J. Chem. Phys.* **59**, 3740 (1973).
- <sup>16</sup>M. Munowitz, R. G. Griffin, G. Bodenhausen, and T. H. Huang, *J. Am. Chem. Soc.* **103**, 2529 (1981).
- <sup>17</sup>X. Feng, Y. K. Lee, D. Sandstrom, M. Eden, H. Maisel, A. Sebald, and M. H. Levitt, *Chem. Phys. Lett.* **257**, 314 (1996).
- <sup>18</sup>M. Hong, J. D. Gross, and R. G. Griffin, *J. Phys. Chem. B* **101**, 5869 (1997).
- <sup>19</sup>U. Haerberlen and J. S. Waugh, *Phys. Rev.* **175**, 453 (1968).
- <sup>20</sup>Y. Ishii, T. Terao, and M. Kainosho, *Chem. Phys. Lett.* **256**, 133 (1996).
- <sup>21</sup>M. H. Levitt, T. G. Oas, and R. G. Griffin, *Isr. J. Chem.* **28**, 271 (1988).
- <sup>22</sup>T. G. Oas, R. G. Griffin, and M. H. Levitt, *J. Chem. Phys.* **89**, 692 (1988).
- <sup>23</sup>Z. Gan, D. M. Grant, and R. R. Ernst, *Chem. Phys. Lett.* **254**, 349 (1996).
- <sup>24</sup>M. Lee and W. I. Goldberg, *Phys. Rev. A* **140**, 1261 (1965).
- <sup>25</sup>A. Bielecki, A. C. Kolbert, and M. H. Levitt, *Chem. Phys. Lett.* **155**, 341 (1989).
- <sup>26</sup>A. Bielecki, A. C. Kolbert, H. J. M. de Groot, R. G. Griffin, and M. H. Levitt, *Adv. Magn. Reson.* **14**, 111 (1990).
- <sup>27</sup>Y. K. Lee, N. D. Kurur, M. Helmle, O. G. Johannessen, N. C. Nielsen, and M. H. Levitt, *Chem. Phys. Lett.* **242**, 304 (1995).
- <sup>28</sup>B.-J. v. Rossum, H. Forster, and H. J. M. de Groot, *J. Magn. Reson.* **124**, 516 (1997).
- <sup>29</sup>C. H. Wu, A. Ramamoorthy, and S. J. Opella, *J. Magn. Reson., Ser. A* **109**, 270 (1994).
- <sup>30</sup>A. Ramamoorthy, C. H. Wu, and S. J. Opella, *J. Magn. Reson., Ser. B* **107**, 88 (1995).
- <sup>31</sup>M. Baldus and B. H. Meier, *J. Magn. Reson.* **128**, 122 (1997).
- <sup>32</sup>G. Metz, X. Wu, and S. O. Smith, *J. Magn. Reson.* **A110**, 219 (1994).
- <sup>33</sup>A. Abragam, *Principles of Nuclear Magnetism* (Clarendon, Oxford, 1961), Vol. 32.
- <sup>34</sup>V. B. Cheng, H. H. Suzukawa, and M. Wolfsberg, *J. Chem. Phys.* **59**, 3992 (1973).
- <sup>35</sup>R. A. Haberkorn, R. E. Stark, H. v. Willigen, and R. G. Griffin, *J. Am. Chem. Soc.* **103**, 2543 (1981).
- <sup>36</sup>A. E. Bennett, Ph.D. thesis, Massachusetts Institute of Technology, 1995.
- <sup>37</sup>Y. Ishii, J. Ashida, and T. Terao, *Chem. Phys. Lett.* **246**, 439 (1995).